

Dry plasma synthesis of MWNT-Pt nanohybrid as an efficient and low-cost counter electrode material for dye-sensitized solar cells

Van-Duong Dao, Ho-Suk Choi*

Department of Chemical Engineering, Chungnam National University, 220 Gung-Dong, Yuseong-Gu, Daejeon 305-764, Korea

Experimental Section

Materials

A Pt precursor solution containing 10 mM $\text{H}_2\text{PtCl}_6 \cdot x\text{H}_2\text{O}$ ($\geq 37.5\%$ Pt basic, Sigma-Aldrich) in iso-propyl alcohol (IPA) (99.5%, Sigma-Aldrich) was first prepared. Pristine multi-walled CNTs were purchased from Hanwha Nano Tech, Korea. FTO glass as a conductive transparent electrode was purchased from Pilkington, USA ($\sim 8 \text{ Ohm}/\square$). These substrates were used after cleaning by sonic treatment in acetone (Fluka). Nonporous TiO_2 paste and ruthenium based-dye (N719) were purchased from Solaronix, Switzerland. The dye was absorbed from a 0.3 mM solution in a mixed solvent of acetonitrile (Sigma-Aldrich) and tert-butylalcohol (Aldrich) with a volume ratio of 1:1. The electrolyte was a solution of 0.60 M 1-methyl-3-butylimidazolium iodide (Sigma-Aldrich), 0.03 M I_2 (Sigma-Aldrich), 0.10 M guanidiniumthiocyanate (Sigma-Aldrich), and 0.50 M 4-tert-butylpyridine (Aldrich) in a mixed solvent of acetonitrile (Sigma-Aldrich) and valeronitrile, with a volume ratio of 85:15.

Synthesis of MWNT-Pt nanohybrid using DPR

Synthesis of MWNT-Pt nanohybrid using DPR was carried out as Scheme 1: The pristine MWNTs were purified by acid treatment [S1] and open-ended in advance by thermal treatment at 470 °C for 30 min [S2]. The MWNTs (100 mg) were added to a solution of H_2PtCl_6 (10 mM) in iso-propanol (20 ml). The mixture was ultrasonicated for 2 hours and then the iso-propyl alcohol was evaporated at 50 °C in a vacuum oven. As a result, the Pt compounds were well intercalated or encapsulated into the MWNTs. For the formation of Pt-NPs, the mixtures of MWNTs with Pt compounds in reactor were treated by an atmospheric pressure plasma (Ar, 200 W for power, 5 lpm for flow rate, 5 mm/s for moving speed, and 30 min for treatment time).

The MWNT-Pt nanohybrid (inside) using DPR was prepared as previous study [S3]. Due to the open-ended structure of the unpurified MWNTs obtained through the thermal

pretreatment [S2], the Pt precursors can be impregnated and trapped inside the MWNTs while removing the solvent at 50 °C in a vacuum. Through the plasma treatment, the Pt ions impregnated into the inside of the MWNTs can be reduced to Pt-NPs. After that, the unpurified MWNT-Pt nanohybrid was mixed with hydrochloric acid (37%). In order to further remove the catalyst impurities, sonication for 1 hour and filtration at least 5 times were performed until the pH of the solution was neutral. The structure of the MWNT-Pt nanohybrid (inside) was obtained and measured by transmission electron microscopy (TEM).

Characterization of MWNT-Pt (DPR) nanohybrid

The structural characterization of the synthesized MWNTs with Pt-NPs was performed by a transmission electron microscope and an energy-dispersive X-ray spectrometer (JEM-2100F, Joel, Japan). The corresponding mass of the Pt-NPs loaded on the nanohybrid was investigated by inductively coupled plasma-atomic emission spectroscopy (Optima 7300 DV, Perkin-Elmer, USA).

Preparation of counter electrodes

The MWNT-Pt nanohybrid powder, prepared by both WPR and DPR, was mixed with a 1 wt% solution of ethyl cellulose (Sigma-Aldrich) in terpineol (Aldrich) by a three-roll miller. The mixtures were coated on the FTO-glass substrates by a doctor blade and dried at 300 °C for 30 min to obtain the MWNT-Pt nanohybrid counter electrodes [S3].

Cyclic voltammetry in I₂+I⁻ system, assembly and measurement of DSCs

The assembly and measurements of the DSCs were carried out as described in a previous study [S3, S4].

Electrochemical impedance spectroscopy (EIS) and Tafel measurements

They were performed as previous study [S5].

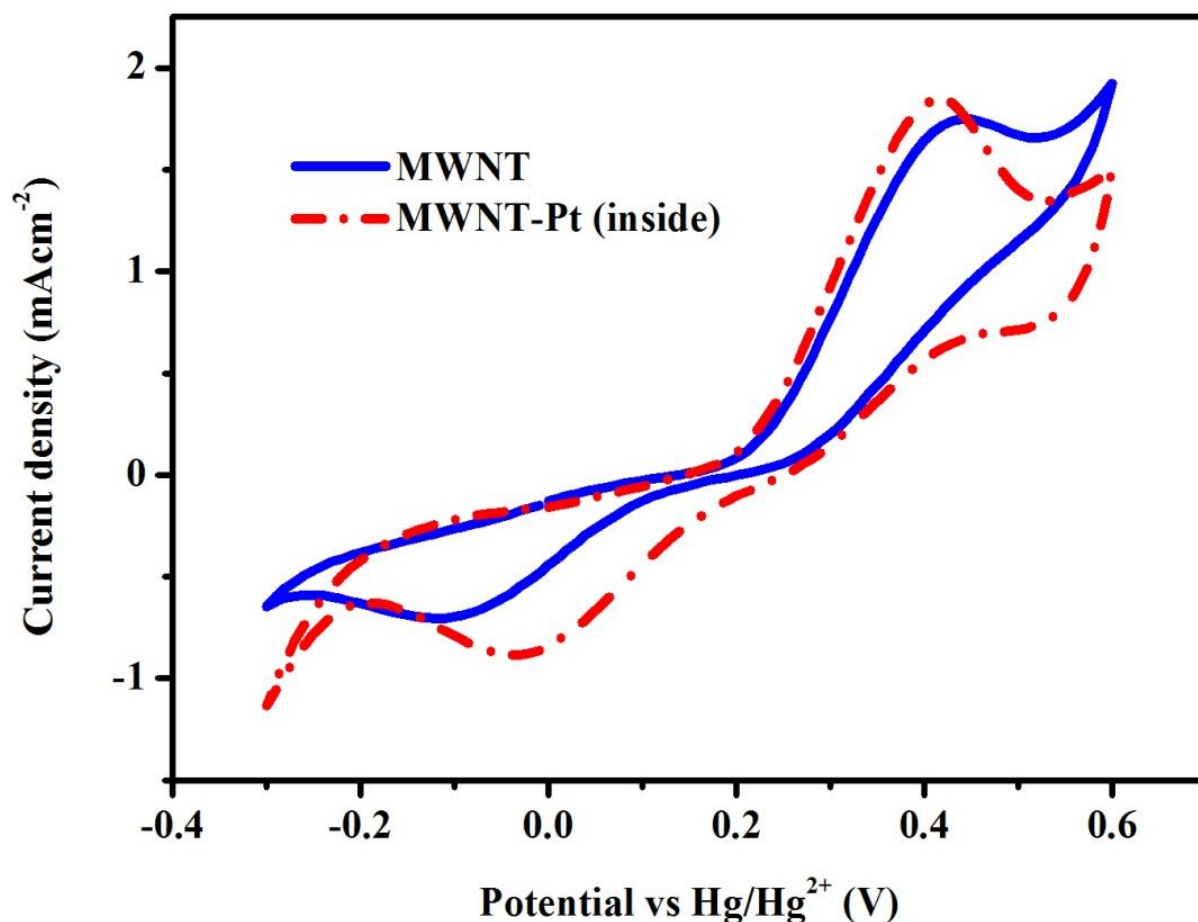


Figure S1. Cyclic voltammograms of MWNT electrode and MWNT-Pt (inside) electrode in 5 mM LiI + I₂ acetonitrile solution containing 0.1 M LiClO₄ as the supporting electrolyte. [I⁻]/[I₂] = 10/1, reference electrode: Hg/Hg²⁺ reference electrode in acetonitrile.

Amount of Pt at the inside of MWNTs is very small, compared with the amount of Pt at the outside of MWNTs. One can first quantify the amount of Pt with the MWNTs having Pt-NPs at both inside and outside of the MWNTs with ICP-MS and then further quantify the amount of Pt with the MWNTs having Pt-NPs at only inside of the MWNTs with the same method. From those two data, one can estimate the amount of Pts at the outside of the MWNTs. The Pt-NPs at the inside of MWNTs also showed the catalytic activity but the catalytic activity was not high enough due to their small amount and inner location. We represented the cyclic voltammograms of MWNT electrode and MWNT-Pt (inside) electrode for comparison in Figure S1.

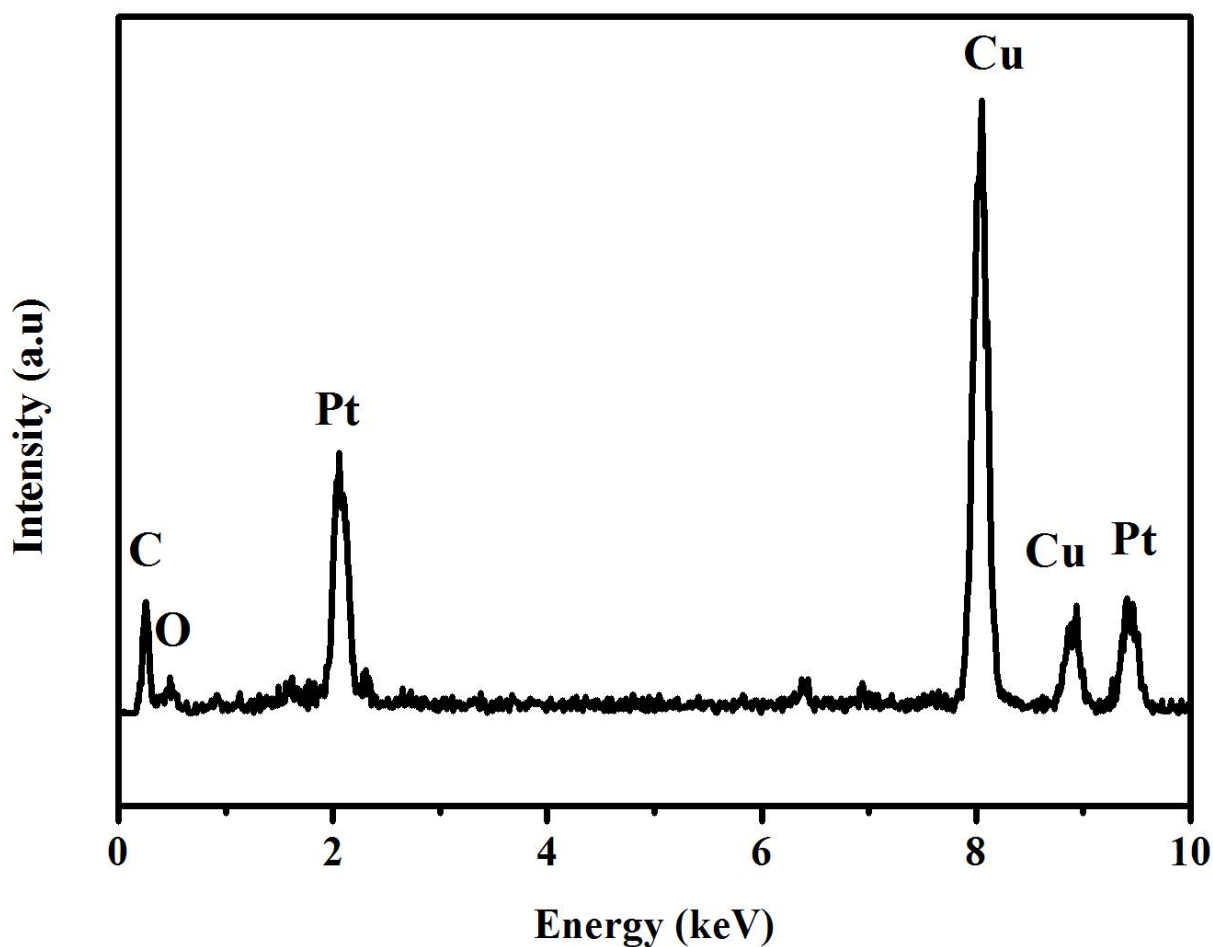


Figure S2. EDS spectra obtained from the all area of TEM image in Fig. 1a treated with the Ar plasma.

Energy dispersive x-ray spectroscopy (EDS), measured during the transmission electron microscopy (TEM) observation in Figure S2, identified the Pt-NPs immobilized on the surface of the MWNTs. The peaks of Pt were observed at 2.1 keV and 9.6 keV, as shown in Figure S2. The other peaks for C, O, and Cu must come from the MWNTs, oxygen-containing functional groups, background grid and system, respectively.

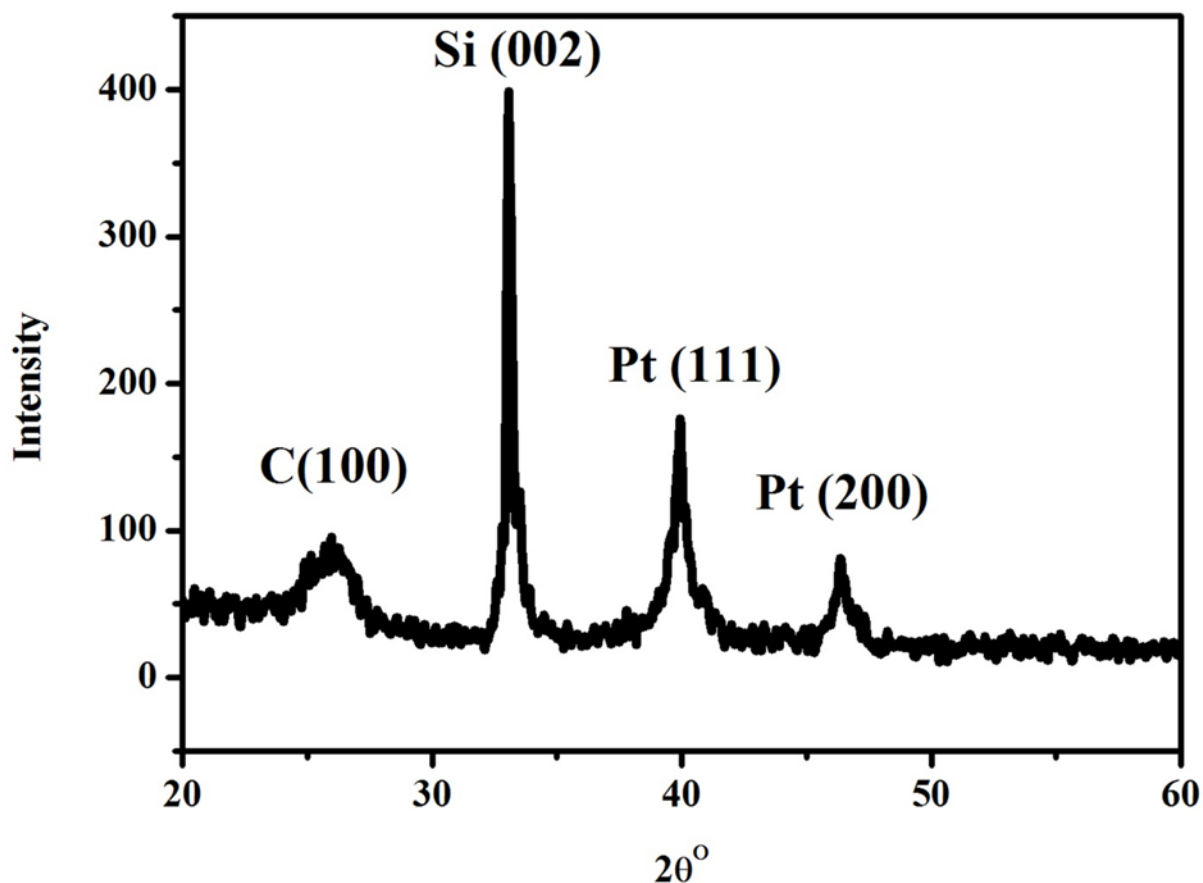


Figure S3. XRD pattern of MWNT-Pt (DPR) nanohybrids on Si wafer substrate.

X-ray diffraction (XRD) of the MWNT-Pt nanohybrid samples on the Si wafer substrate was performed on a Rigaku D/MAX-RC (12kW), as shown in Fig. S3. The single broad diffraction peak at around $2\theta=26.46^\circ$ belongs to the MWNT support, and $2\theta=33^\circ$ belongs to the Si wafer substrate. All XRD patterns of the MWNT-Pt nanohybrid sample exhibit the characteristic diffraction peaks of Pt (111) at $2\theta=39.7^\circ$, and Pt (200) at $2\theta=46.2^\circ$ indicating that Pt is present in the face centered cubic (FCC) phase.

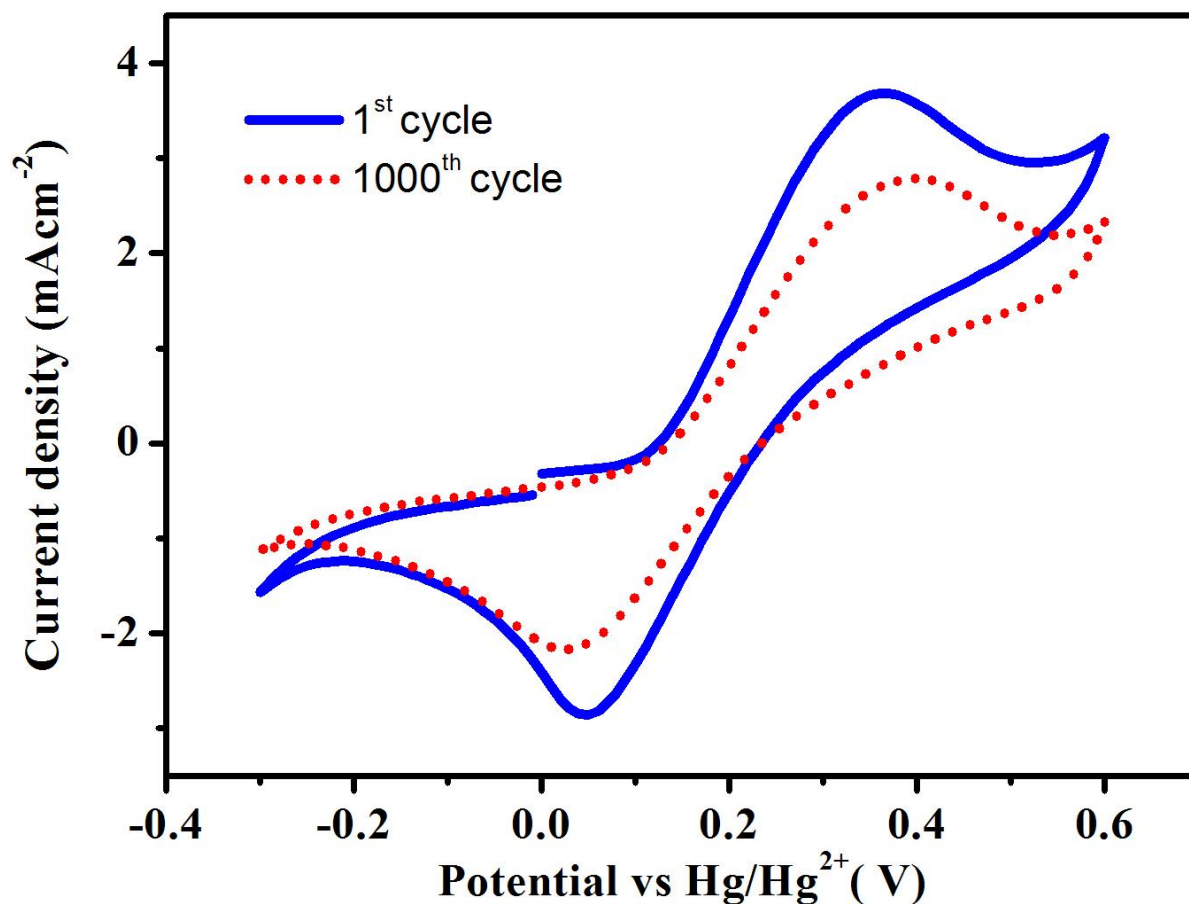


Figure S4. Current-voltage curves over time for the redox system with the MWNT/Pt (DPR) working electrode and Pt-mesh counter electrode.

The stability of the electrode materials is also important for applications. The DSC with the MWNT-Pt (DPR) as counter electrode (CE) showed a reasonable stability. This stability was confirmed by the stability of the current-voltage curves over time for the redox system with the MWNT-Pt (DPR) working electrode and Pt mesh CE (Figure S4). Slight detachment of Pt NPs from the surface of MWNT was observed after 1000th cycle. However, the catalytic activity of MWNT-Pt (DPR) even measured after 1000th cycle was almost equivalent to that of MWNT-Pt (WPR) measured at first time.

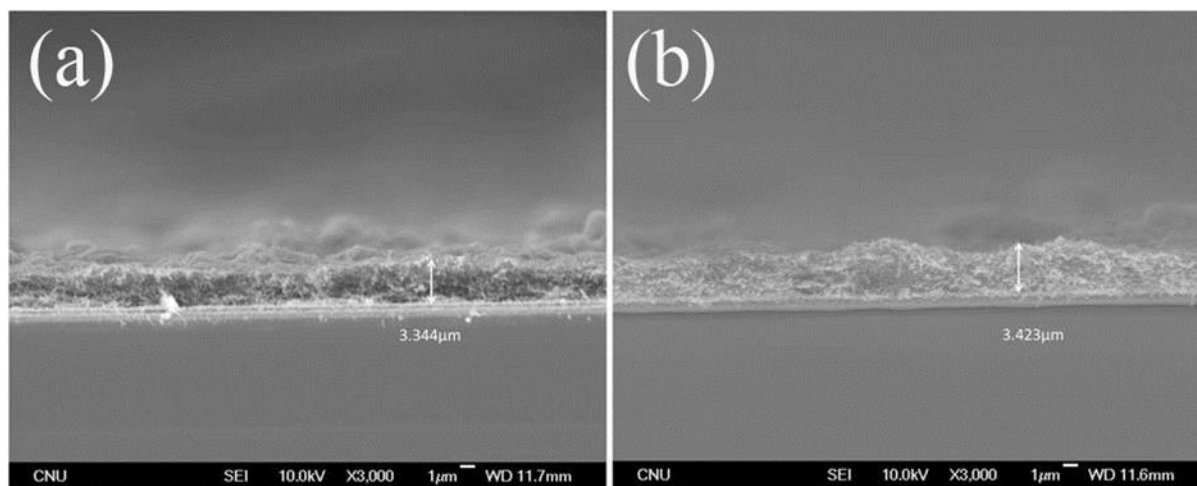


Figure S5. SEM images of electrode films on FTO glass substrate (cross-section), showing the thickness of the films. a) MWNT-Pt (WPR) [S3], b) MWNT-Pt (DPR).

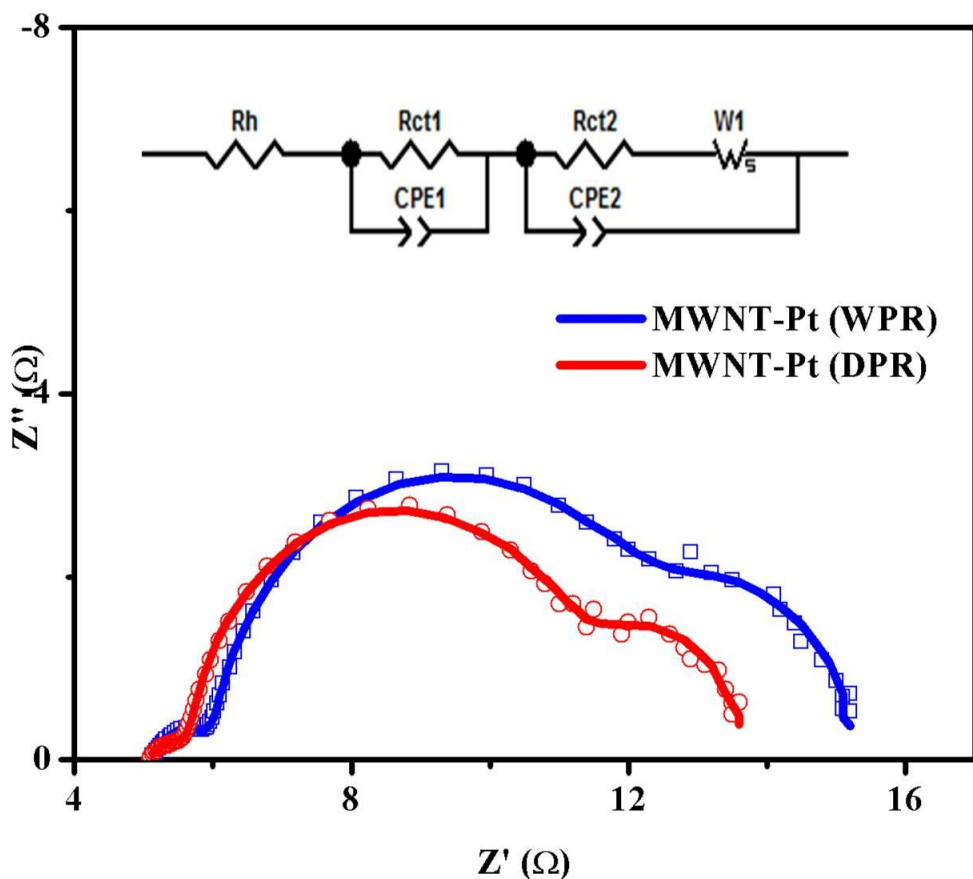


Figure S6. Nyquist plots of two DSCs equipped with MWNT-Pt (WPR) and WMNT-Pt (DPR) CEs. The inset image shows the equivalent circuit diagram used to fit the observed impedance spectra. R_h : ohmic serial resistance; R_{ct1} : charge-transfer resistance of CE; CPE1: constant phase element of CE; R_{ct2} : charge-transfer resistance of working electrode; CPE2: constant phase element of working electrode and W_s : Warburg impedance.

Table S1. Impedance parameters of DSCs equipped with two MWNT-Pt CEs, estimated from the impedance spectra and equivalent circuit shown in Figure S6.

CE	R_h (Ωcm^2)	R_{ct1} (Ωcm^2)	CPE1-T (mFcm^{-2})	CPE1-P	R_{ct2} (Ωcm^2)	W_s			CPE2-T (mFcm^{-2})	CPE2-P
						R	T	P		
WPR	2.51	0.44	1.35	0.75	3.05	1.45	0.42	0.5	4.49	0.95
DPR	2.48	0.32	7.76	0.60	2.67	1.21	0.6	0.5	4.49	0.95

The EIS data of full cells assembled with two CEs were shown in Figure S6 and Table S1. The EIS of DSC was performed under constant light illumination (100 mWcm^{-2}) biased at open-circuit condition. The measured frequency range was 100 kHz to 100 mHz with perturbation amplitude of 10 mV [S6]. We found that the R_{ct} of the MWNT-Pt (DPR)-coated electrode was as small as $0.32 \text{ }\Omega\text{cm}^2$, while the MWNT-Pt (WPR)-coated electrode was $0.44 \text{ }\Omega\text{cm}^2$. The value of the constant phase element ($\text{CPE1} = (\text{CPE1-T})^{-1} (\text{j}\omega)^{-(\text{CPE1-P})}$) of the CE also confirms that the active surface area of MWNT-Pt (DPR)-coated electrode is larger than that of the MWNT-Pt (WPR)-coated electrode. Indeed, the value of CPE1-T, 7.76 mFcm^{-2} , for the MWNT-Pt (DPR)-coated electrode is greater than 1.35 mFcm^{-2} of the MWNT-Pt (WPR)-coated electrode as shown in Table S1. A larger CPE1-T means an increase in the active surface area. The porosity value (CPE1-P) for two CEs are also listed in Table S1. A decrease of CPE1-P means an increase in the porosity. The value of CPE1-P, 0.60, for the MWNT-Pt (DPR)-coated electrode is smaller than that of the MWNT-Pt (WPR)-coated electrode, viz. 0.75. The reduction of the total internal resistance due to the decrease in the charge-transfer resistance is the cause of the increase in the fill factor (FF) of the DSCs [S3, S7], which confirms the increase in the conversion efficiency. The decrease rate of charge transfer resistance, however, was about 30 % from $0.44 \text{ }\Omega\text{cm}^2$ to $0.32 \text{ }\Omega\text{cm}^2$ between two full cells, which is smaller than 57 % from $0.28 \text{ }\Omega\text{cm}^2$ to $0.12 \text{ }\Omega\text{cm}^2$ between two dummy cells. A full cell is composed of working electrode, electrolyte, counter electrode and their interfaces. The charge transfer resistance in other part like working electrode can be a rate-limiting step for the sequential charge transfer in a full cell. This can explain the reason why the photovoltaic efficiency is only slightly improved in the DSC with the MWNT-Pt (DPR). Since, however, the electrochemical measurements using symmetric dummy cells show obvious improvement, the DSC with the MWNT-Pt (DPR) counter electrode has high potential to be able to further improve the cell efficiency if we can reduce the charge transfer resistances in other parts.

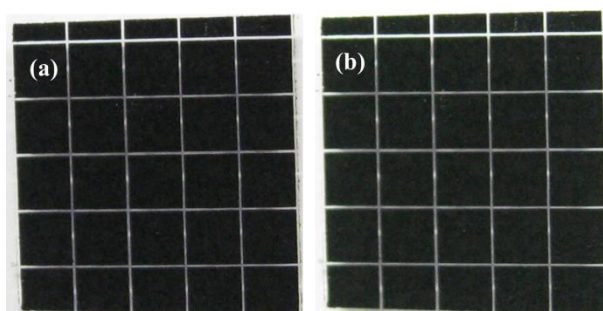


Figure S7. Result of adhesion test (ASTM D3359-B); (a) before and (b) after testing.

The adhesion of the MWNT-Pt (DPR) on the TCO glass was very stable as shown in Figure S7. The test result was 5B, which meant stable adhesion of coated layer.

References

- [S1] V. Lordi, N. Yao, J. Wei, *Chem. Mater.*, 2001, **13**, 733.
- [S2] K. Baba, T. Kaneko, R. Hatakeyama, K. Motomiyac, K. Tohji, *Chem. Commun.*, 2010, **46**, 255
- [S3] V. D. Dao, S. H. Ko, H. S. Choi, J. K Lee, *J. Mater. Chem.*, 2012, **22**, 14023
- [S4] V. D. Dao, S. H. Kim, H. S. Choi, J. H. Kim, H. O. Park, J. K. Lee, *J. Phys. Chem. C* 2011, **115**, 25529.
- [S5] V. D. Dao, H. S. Choi, *Electrochimica Acta*, 2013, **93**, 287-292
- [S6] D. W. Zhang, X. D. Li, S. Chen, F. Tao, Z. Sun, X. J. Yin, S. M. Huang, *J. Solid-State Electrochem.*, 2010, **14**, 1541
- [S7] V. D. Dao, H. S. Choi, K. D. Jung, *Materials Letters* 2013, **92**, 11-13.